

Measurements of Phase Response in an Oscillatory Reaction and Deduction of Components of the Adjoint Eigenvector

Ian Millett, William Vance, and John Ross*

Department of Chemistry, Stanford University, Stanford, California 94305

Received: June 21, 1999; In Final Form: August 16, 1999

We present the first experiments that use the phase response method to determine components of the adjoint eigenvector (of the Jacobian matrix of the linearized system) of an oscillating reaction system. The Briggs–Rauscher reaction was studied near a supercritical Hopf bifurcation. Phase response curves for I^- and Mn^{2+} have been determined, and from them corresponding components of the adjoint eigenvector have been deduced. The relative magnitudes and difference in arguments of these components agree reasonably well with those from a reduced model of the Briggs–Rauscher reaction, whereas agreement with results from quenching experiments is mixed.

I. Introduction

Several approaches have been suggested and analyzed for the determination from experiments, rather than the hypothesizing, of reaction pathways and mechanisms in complex kinetic systems.^{1–10} Of great interest in this regard are oscillatory reactions, which may be classified according to the type of feedback mechanism.¹ In ref 5 we listed 13 different experiments from which information may be deduced about the reaction mechanism. Three of these measurements are phase response to a discrete perturbation, external periodic perturbations, and quenching. In the first, a perturbation in the concentration of a chemical species is introduced into the oscillatory reaction system and the phase response of a (test) species is measured. In experiments in which the concentration of one of the species in the system is varied periodically by external means, the response of the phase of a test species is measured, say for example in the fundamental entrainment band. In quenching experiments^{11,12} changes in concentrations of a species, increases or decreases, are made by trial until at an empirically determined phase of the oscillations there results a temporary quenching of the oscillations. As in the previous two measurements, a test species is monitored to detect when a quenching has occurred. For systems near a supercritical Hopf bifurcation, from stationary to oscillatory temporal variations of concentrations, Hynne et al.¹² have derived the relation of the adjoint eigenvector (corresponding to a pure imaginary eigenvalue) to quenching experiments. (Adjoint eigenvectors are left eigenvectors of the Jacobian matrix for the system linearized about the stationary state.) The adjoint eigenvectors provide restrictions on the components of the Jacobian matrix, and thus indirectly on the reaction mechanism, and may also be compared directly with predictions from proposed model systems.

Vance and Ross¹³ have shown theoretically that essentially the same information about adjoint eigenvectors as obtained from quenching experiments can also be derived from phase response and periodic perturbation experiments, which require far fewer empirical determinations of appropriate conditions. In particular for the perturbation of a given species, the amplitude and zero crossing (with positive slope) of a phase response function equal the magnitude and argument, respectively, of the corresponding component of the adjoint eigen-

vector. Of great interest for the classification of oscillators is the connection between phase response to the category of oscillator; some details of this relation have been developed in ref 4.

In this study, we selected the Briggs–Rauscher reaction¹⁴ for investigating phase response. It was chosen for several desirable aspects: it is one of the oldest oscillating reactions, many features of its mechanism have been established, and an extensive series of quenching experiments have been carried out on it. The reaction involves the iodate oxidation of malonic acid in an acidic media of hydrogen peroxide and is catalyzed by Mn^{2+} . We measure phase responses near a Hopf bifurcation; concentration perturbations are made with I^- and separately with Mn^{2+} . The measurements are somewhat complicated by the slow relaxation of the perturbed oscillatory reaction system near a Hopf bifurcation.

The experimental setup is discussed in section II; the measurements and their results are reported in section III; comparisons of the experiments are made in section IV. In the comparison with calculations we use a tractable model of the Briggs–Rauscher reaction and calculate phase response curves. Agreement with the experiments is good. The other comparison is made with deductions from quenching measurements and there the agreement is mixed.

II. Experimental Section

A. Equipment. We investigated the original version of the Briggs–Rauscher oscillating reaction in which malonic acid is oxidized by iodate and hydrogen peroxide in acidic media with manganous ions acting as a catalyst. Three feed solutions were used, hydrogen peroxide, potassium iodate, and a combination of manganous sulfate and hydrogen peroxide, respectively. Each feed solution was acidified using perchloric acid; the concentration of H^+ ion in feeds was the same as the desired concentration in the reactor, 0.0131 M.

The reaction was carried out in a Pyrex glass CSTR of volume 49.5 mL, which was surrounded by a cooling jacket maintained at a constant temperature (21 °C). Reactants were kept in the water bath used for the jacket and fed into the reaction chamber through 50 μ L pipets using peristaltic pumps (Ismatec IPS-4).

Due to the much higher concentration of hydrogen peroxide than the other reactants in the feed stream, we were concerned about possible mixing effects if only one feed were used. We therefore split the feed of H_2O_2 into two inputs positioned at opposite sides of the reactor. The system was perturbed by injecting small aliquots of known concentration into the reactor, using a 200 μL gastight Hamilton syringe. A triggering mechanism recorded the exact time a perturbant was injected.

The reaction was monitored with a double junction iodide-selective electrode (Cole-Parmer H-27502-23). The logarithmic response of the electrode makes quantitative measurements of small concentration changes difficult; we used the output directly as a qualitative measure (this is sufficient for phase response studies). The response time of the electrode is much less than the period of oscillations. Experiments were run by a 486/33 IBM-compatible computer running Windows 3.1. Custom programs interfaced with a Data Translations DT-2805 A/D-D/A board.

B. Operating Conditions. We used the same input concentrations as employed by Vukojevic et al.¹⁵ in their quenching studies. The mixed flow concentrations were: $[\text{H}^+] = 0.0131 \text{ M}$, $[\text{Mn}^{2+}] = 2.22 \times 10^{-3} \text{ M}$, $[\text{IO}_3^-] = 6.24 \times 10^{-2} \text{ M}$, $[\text{H}_2\text{O}_2] = 0.158 \text{ M}$, and $[\text{MA}] = 2.80 \times 10^{-2} \text{ M}$. All reagents were commercial analytical grade. Due to the decrease in molarity of the hydrogen peroxide solution with time, we calibrated a stock solution of hydrogen peroxide against a standardized permanganate solution before each experimental run.

III. Measurements and Results

A. Location of a Hopf Bifurcation. With the inflow species and their concentrations listed in section II we located a Hopf bifurcation in the Briggs-Rauscher reaction at an inflow rate of 11.4 mL/min, which corresponds to a specific flow rate of 0.0038 s^{-1} . Above a minimum level of stirring of about 300 rpm the location of the bifurcation point is independent of the rate of stirring. In ref 11 the bifurcation was reported to be at 0.00423 s^{-1} , which is within about 10% of our result. A contributing cause to this difference is the long relaxation time near the Hopf bifurcation.

B. Period of the Oscillations. The period of the oscillations at a specific flow rate of 0.00391 s^{-1} , which is close to the Hopf bifurcation value, is determined, by repeated measurements of the time interval between one and the next peak in the concentration of iodide ion, to be $T = 26.6 \pm 0.48 \text{ s}$. (This agrees very well with the experimental result in ref 15 of 27.3 s.) The sampling rate of iodide ion concentration is 0.4 s and thus the uncertainty in the period is about one "bin". The oscillations are nearly sinusoidal as is shown in Figure 1.

C. Transients and Long Relaxations. Near the Hopf bifurcation the system requires a very long time, that is hours, to relax from a perturbation. This is illustrated in Figure 2 and discussed in the caption.

D. Phase Resetting with Perturbations of Iodide Ion. A phase shift is most conveniently defined in terms of an event surface. We use the minimum of the response of the iodide-selective electrode to define an event; the phase on the event surface is taken to be zero. A phase resetting experiment consists of perturbing the oscillator at a selected phase, letting the system relax, and monitoring the shift (in time) of marker events. If we denote the elapsed times from the marker event that immediately preceded the perturbation to subsequent marker events by t_k , $k = 1, 2, \dots$, then after n minima of the response of the electrode have occurred, the phase shift is approximated by $n - t_n/T$.

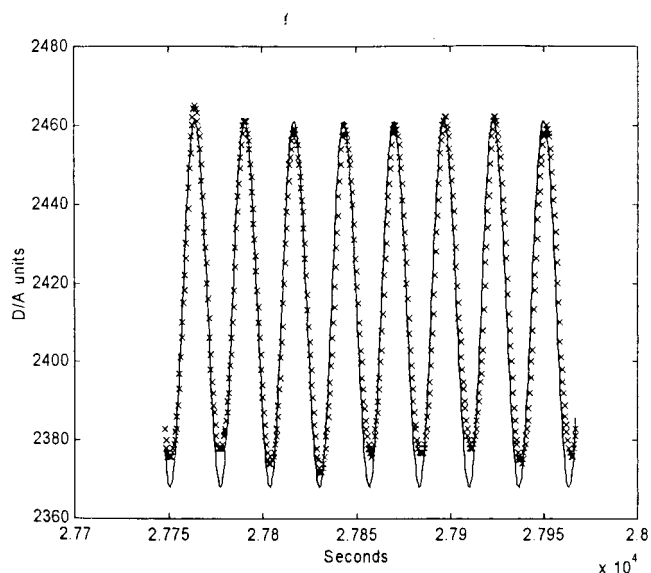


Figure 1. Autonomous oscillations of the Briggs-Rauscher reaction under the experimental conditions described in section II. The experimental points are marked by the symbol \times ; for comparison, a sinusoid of period 26.6 s is plotted as the solid line.

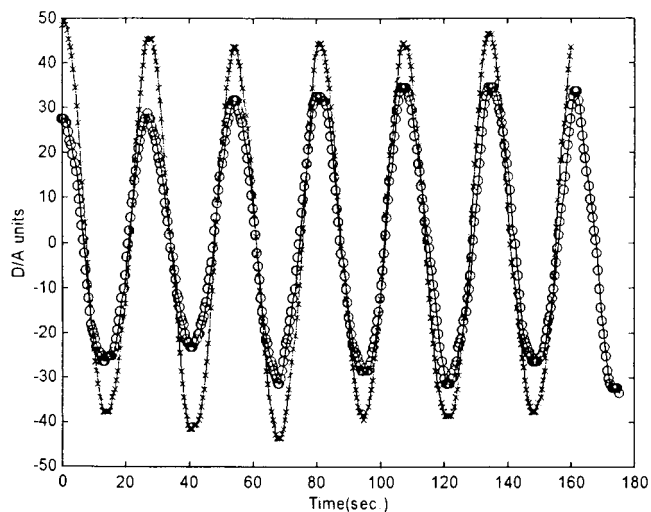


Figure 2. An example of long transients encountered in the system. The flow rate was increased by 1% to a final value of 0.00391 s^{-1} . The first curve, marked by circles, was collected 1.5 h after making the increase; the second curve, marked by the symbol \times , was collected 4 h after making the increase. During the intervening 2.5 h, the period of oscillations remained constant, while the amplitude increased by 30%.

The perturbations made with iodide ions consisted of injecting 200 μL of a $6.92 \times 10^{-4} \text{ M}$ solution of KI in the reactor; the resulting perturbation strength in iodide ion concentration was $2.80 \times 10^{-6} \text{ M}$, which induced a small but measurable shift in the phase of the oscillations. Figure 3 shows such a perturbation applied at a phase of the unperturbed system of $\theta = 0.84 = 302^\circ$, marked by a cross. The diamond prior in time to the cross serves as a reference point; the diamonds after the cross serve for measurement of the phase shift. We used the third minimum after the perturbation to measure a phase shift of 0.9s.

The phase response function, using the third minimum after the perturbation, is shown in Figure 4: the circles are the measured phase shifts $\Delta\theta$ at various phases of the unperturbed system, θ . We expect¹³ the induced phase shift to depend linearly on the cosine of (constant $+2\pi\theta$). The solid line is a fit of this form to the measurements

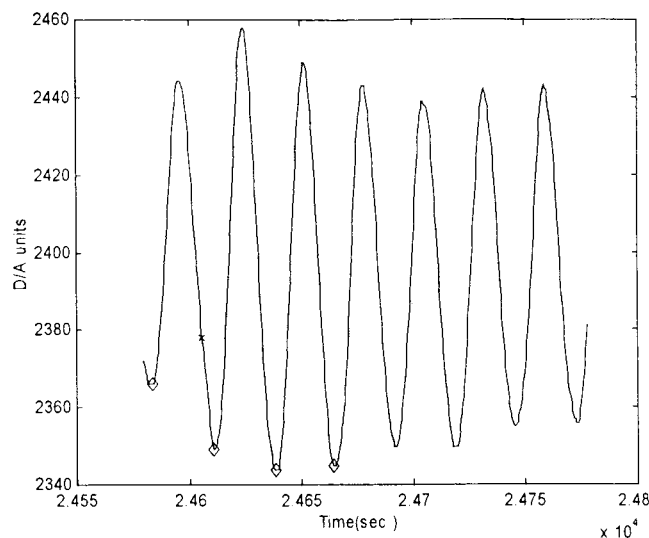


Figure 3. Time series for a perturbation in I^- at phase $\theta = 0.84$. The symbol \times marks the location of the perturbation and the diamonds identify marker events. The event prior to the perturbation acts as the phase reference point; subsequent events are used to calculate the phase shift.

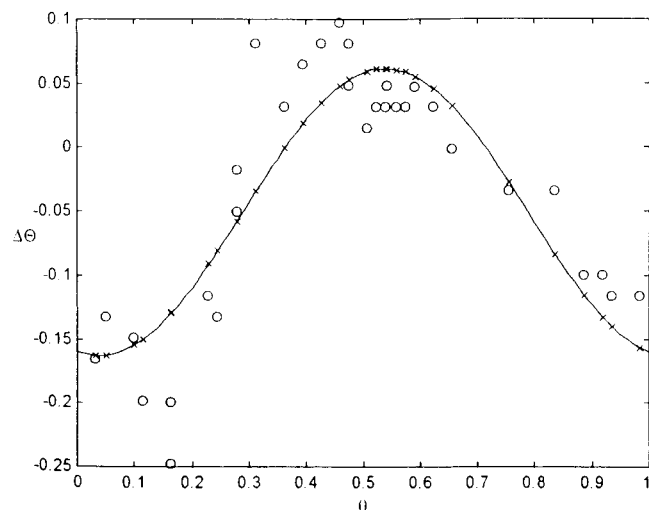


Figure 4. Plot of the experimentally determined and the fitted (eq 1) phase response function for species I^- . Phase shifts were calculated using the third minimum after the I^- perturbation. Open circles denote measured phase shifts, and the symbol \times denotes values of the fitted equation at experimental perturbation phases.

$$\Delta\Theta = -0.0508 + 0.112 \cos(2.90 + 2\pi\theta) \quad (1)$$

with a standard deviation of 0.0080.

If we use the fourth, instead of the third, minimum for the measurement of the induced phase shift then we obtain quite similar results, with the fit of an equation of the form somewhat worse, that is a standard deviation of 0.0105.

E. Phase Resetting with Perturbations of Manganese Ion.

The perturbation consisted of the addition of 200 μL of 0.0133 M solution of MnSO_4 to the reactor; the resulting perturbation strength in manganese ion concentration was 5.38×10^{-5} M. This perturbation was sufficient to produce a small but measurable phase shift in the oscillations. Figure 5 gives the phase shifts (circles), using the third minimum after the perturbation, for various values of the phase of oscillation of the unperturbed system. The solid line is the fit of an equation analogous to eq 1:

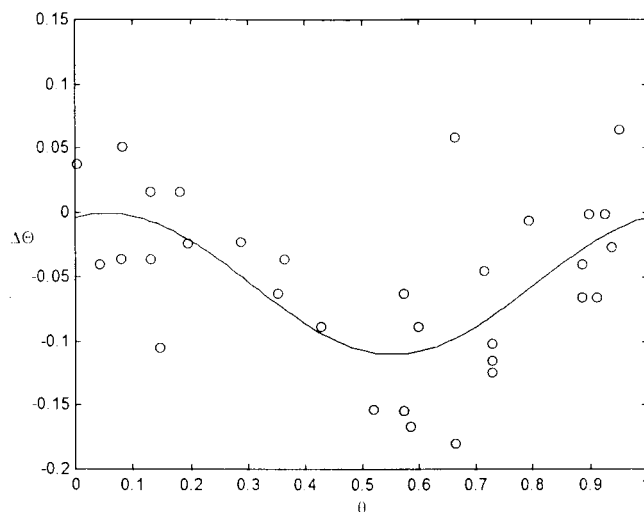


Figure 5. Plot of the experimentally determined and the fitted (eq 2) phase response function for species Mn^{2+} . As for I^- , phase shifts were calculated using the third minimum after the Mn^{2+} perturbation. Open circles denote measured phase shifts.

$$\Delta\Theta = -0.0554 + 0.0548 \cos(5.94 + 2\pi\theta). \quad (2)$$

IV. Comparison of Experimental Results with Predictions from a Model and Quenching Experiments

In this section we compare our experimental results with a model of the Briggs–Rauscher reaction and also with quenching experiments of Vukojevic et al.¹⁵ In addition, we report results for the adjoint eigenvector based on numerical simulations of phase resetting and compare them with exact results based on the Jacobian matrix.

A. Turanyi-Furrow Model of the Briggs-Rauscher Reaction.

We used the model of the Briggs–Rauscher system described Turanyi and Furrow.^{16,17} (The adopted values for the rate constants are close to those used in ref 15 for the TF model.) The TF model is a simplified version of several more complicated models: several reactions were eliminated using sensitivity analysis (e.g. the reaction of Mn^{2+} with H_2O_2). In this mechanism, the species $\text{Mn}(\text{OH})^{2+}$, iodomalonic acid, and oxygen are considered inert reaction products. We held three species fixed at their input concentrations: $[\text{IO}_3^-] = 6.24 \times 10^{-2}$ M, $[\text{H}_2\text{O}_2] = 0.158$ M, and $[\text{MA}] = 2.80 \times 10^{-2}$ M.

We adjusted the values of the rate constants of this model to reproduce the observed the Hopf bifurcation value and period of oscillation as closely as possible, see Table 1. [We used values given by Vukojevic et al. in ref 15 as initial values; most of the best-fit values are within a factor of 2 of the initial values.] The rate of a reaction is described through mass action kinetics in which all species shown are included. The unit of concentration is $\text{M} = \text{mol dm}^{-3}$, and the unit of time is seconds. For clarity, units for the rate coefficients are omitted in Table 1.

The Hopf bifurcation point occurs for a specific flow rate of 0.00421 s^{-1} ; this value is within 10% of the observed experimental value of 0.0038 s^{-1} . The period of oscillations 18.3 s, which is roughly two-thirds of the experimentally observed 26.6 s.

B. Interpretation of Phase Response Experiments. For systems near a Hopf bifurcation, both phase response and quenching experiments yield components of the adjoint eigenvector ζ^* corresponding to the pure imaginary eigenvalue $i\omega$ of the Jacobian matrix. [More specifically, the adjoint eigenvector is the left eigenvector of the deterministic system linearized about the stationary state at the Hopf bifurcation point.] The phase response procedure involves perturbing the

TABLE 1: Turanyi and Furrow Model for the Briggs–Rauscher Reaction as Used in the Simulations

reaction step	rate coefficient
$2\text{H}^+ + \text{I}^- + \text{IO}_3^- \rightarrow \text{HOI} + \text{HIO}_2$	1500
$\text{H}^+ + \text{HIO}_2 + \text{I}^- \rightarrow 2\text{HOI}$	5×10^9
$\text{HOI} + \text{I}^- + \text{H}^+ \rightarrow \text{I}_2 + \text{H}_2\text{O}$	1×10^9
$\text{I}_2 + \text{H}_2\text{O} \rightarrow \text{HOI} + \text{I}^- + \text{H}^+$	3×10^{-3}
$\text{HIO}_2 + \text{IO}_3^- + \text{H}^+ \rightarrow 2\text{IO}_2^* + \text{H}_2\text{O}$	5×10^5
$2\text{IO}_2^* + \text{H}_2\text{O} \rightarrow \text{HIO}_2 + \text{IO}_3^- + \text{H}^+$	3×10^7
$\text{IO}_2^* + \text{Mn}^{2+} + \text{H}_2\text{O} \rightarrow \text{HIO}_2 + \text{Mn}(\text{OH})^{2+}$	229
$\text{I}_2 + \text{MA} \rightarrow \text{IMA} + \text{I}^- + \text{H}^+$	8
$\text{HOI} + \text{H}_2\text{O}_2 \rightarrow \text{I}^- + \text{H}^+ + \text{O}_2 + \text{H}_2\text{O}$	35

k th species of an oscillating system with a given amplitude perturbation ϵ_k and determining the asymptotic phase shift. (The perturbation may last one oscillation period; see ref 13 for details). This is carried out for sufficiently many points along the limit cycle to determine a curve. In contrast, the quenching procedure involves searching for the optimal phase ϕ_k and perturbation strength q_k for the k th species so as to temporarily stop or quench oscillations.¹⁸

For phase response experiments, a plot of phase shifts against the phases of the oscillator at which the perturbation commenced yields the phase response curve (PRC). The PRC is sinusoidal for systems close to Hopf bifurcations and can be fit to $a_k + b_k \cos(\theta_k + 2\pi\theta)$. The amplitude b_k of the sinusoid is proportional to the perturbation strength ϵ_k . In experiments this proportionality is used by adjusting the strength to give an observable phase shift for a given perturbation species. In contrast to the PRC of phase resetting experiments, quenching experiments yield a single point, (q_k, ϕ_k) .

There is a direct relation between the PRC for a particular perturbation species and the corresponding component of the adjoint eigenvector written in polar form $\zeta_k = r_k \exp(i\psi_k)$: the magnitude r_k and the argument ψ_k are equal to the amplitude b_k and the phase offset θ_k , respectively. This assumes that the experimentally determined amplitude of PRC has been divided by the strength of perturbation ϵ_k . Similarly for quenching data, the amplitude and argument of the adjoint eigenvector are equal to $1/q_k$ and $-\phi_k$, respectively.

To demonstrate the applicability of the phase response method to complex systems, we simulated phase shift measurements for the above TF model. We took the reduced flow rate to be 1% beyond the bifurcation point; this choice yielded nearly sinusoidal oscillations. As in our experiments, the maximum in $[\text{I}^-]$ was chosen as the marker and the third maximum following the perturbation was used to calculate the phase shift. The phase response curve for I^- is shown in Figure 6. Similar curves were obtained for each of the other six species; components of the adjoint eigenvector were obtained from the best sinusoidal fit to the simulation points. A comparison of these values with those of the exact adjoint eigenvector of the Jacobian (evaluated at the Hopf bifurcation point) is given in Table 2. Extremely good agreement is found between each of the elements.

This close agreement may be surprising in light of the original derivation of the phase response curve for systems near Hopf bifurcations, which is based on asymptotic phase shifts.¹³ Under the conditions chosen, the TF model exhibits extremely slow relaxation in the plane of oscillation: the eigenvalue associated with the slow mode (in the plane of oscillation) is 0.0019, which implies that over 35 oscillations are needed for a perturbed orbit to return to the limit cycle and establish an asymptotic phase shift.

The explanation for this behavior may be described briefly. In an n -dimensional system close to a Hopf bifurcation,

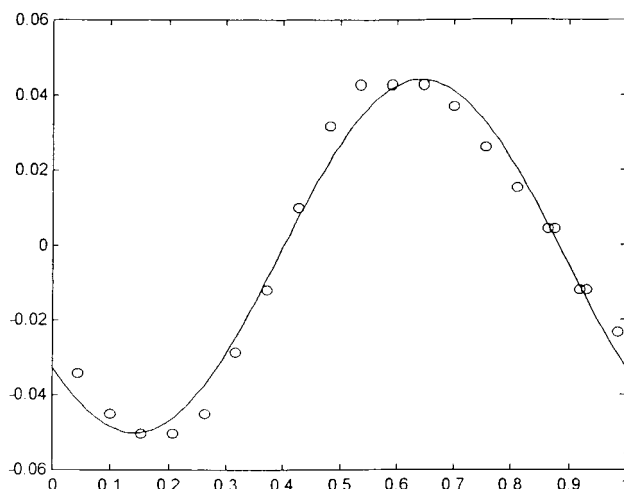


Figure 6. Plot of the simulated phase shifts, denoted by circles, and the fitted equation, denoted by a solid line, for perturbations in I^- . Perturbations increased the concentration of I^- in the reactor by 5×10^{-9} M. The fitted equation is $\Delta\Theta = -0.0030 + 0.047 \cos(2.25 + 2\pi\theta)$.

TABLE 2: Components of the Adjoint Eigenvector for the TF Model Determined from the Jacobian Matrix and from Simulated Phase Shifts (r and ψ are defined in section IV.b)

	TF model: Jacobian matrix		TF model: phase response simulation	
	r	ψ (deg)	r	ψ (deg)
I^-	1	128.9	1	128.9
I_2	0.77	178.6	0.73	178.8
HOI	0.37	-150.7	0.35	-149.1
HIO_2	2.38	-89.4	2.31	-87.2
Mn^{2+}	0.0024	-0.3	0.0025	1.7
H^+	0.00018	14.5	0.00016	17.2
IO_2^*	1.26	-89.3	1.25	-88.9

relaxation to the limit cycle initially occurs along a fast direction, an $n-2$ -dimensional strong stable manifold, which projects a perturbation onto the plane of oscillation. Subsequent slow motion occurs in the plane of oscillation; all points that evolve to the same point on the limit cycle determine an one-dimensional weakly stable manifold. These stable manifolds, weak and strong, determine how perturbations affect the phase of a point on the limit cycle. A small perturbation either advances or retards the phase according to whether the new state is on the stable manifold of a point in advance of or behind the initial one. As derived in Vance and Ross,¹³ the (asymptotic) phase shift along the limit cycle induced by a small perturbation may be expressed in terms of the adjoint eigenvectors ζ^* and $\bar{\zeta}^*$. If we neglect slow relaxation and use an event determined by a test species to define the phase, we can also approximate the resulting experimentally measured phase response curve in terms of ζ^* and $\bar{\zeta}^*$. Adding slow relaxation to the system makes the (complex) constant terms that multiply the eigenvectors become time dependent (on a time scale $t_1 = \mu t$, where μ is a measure of the distance to the Hopf bifurcation). Hence, once a system has relaxed onto the plane of oscillations (typically after a few oscillations), the measured short-time phase shifts accurately determine the adjoint eigenvector. In this procedure it is necessary to use the same number of oscillations to measure the phase shift for all perturbed species. The independence of the phase response method from long time behavior gives the experimenter considerable flexibility in choosing the number of oscillations used to calculate phase responses, and by this the signal-to-noise ratio.

TABLE 3: Comparison of the I^- and Mn^{2+} Components of the Adjoint Eigenvector Measured by Phase Resetting Experiments, by Simulated Phase Shifts on the Turanyi and Furrow Model (Table 1), and by Quenching Experiments of Vukojevic et al. (r and ψ are defined in section IV.b)

	$\psi(Mn^{2+}) - \psi(I^-)$	$r(Mn^{2+})/r(I^-)$
experimental phase resetting	174	0.0073
Turanyi and Furrow model	231	0.0024
experimental quenching	229	0.0271

C. Comparison with Quenching Experiments. We present a comparison of the argument and magnitude of the two components of the adjoint eigenvector that we obtained through experimental phase shift experiments, I^- and Mn^{2+} , with results for quenching experiments and calculations on the TF model, Table 3. We see that the argument of the component for Mn^{2+} leads that for I^- by 3 rad ($=172^\circ$) for experimental phase resetting and by 4 rad ($=229^\circ$) for both the TF model and quenching experiments. This difference may be due in part to the noisy PRCs of the phase shift experiments (see Figures 4 and 5). The comparison between the experiments and the TF model is reversed for the relative magnitudes of the I^- and Mn^{2+} components of the adjoint eigenvector. In this case, results for phase shift experiments differ from the TF model by a factor of 3; whereas, quenching experiments yield a result that differs by over an order of magnitude.

V. Discussion and Conclusion

In this paper we have demonstrated for the first time how experimental phase response experiments can be used to determine components of the adjoint eigenvector (of the Jacobian matrix of the linearized system). These components are closely related to the kinetics of the system and place restrictions on the mechanism and values of the rate constants. We have determined two components, corresponding to I^- and Mn^{2+} , for the Briggs–Rauscher oscillatory reaction and compared these with experimental quenching results and with a simplified model for the system.

Our main conclusion is the ease and accuracy of using phase resetting experiments to determine the adjoint eigenvector. The experimenter only needs to adjust the magnitude of perturbation for each species so that a measurable phase shift is observed; phase shifts from short time series are sufficient to determine components of the adjoint eigenvector. In contrast, the quenching method has exacting requirements: for each species the

experimenter needs to find the correct phase and magnitude of a perturbation that quenches oscillations; this requires observation of long transients and numerous trials.

Based on limited data, we find reasonably good agreement between our experimental results and a reduced model of the Briggs–Rauscher reaction, the TF model (with rate constants adjusted to give a Hopf bifurcation and oscillation frequency that are close to those of the experiments). A comparison of our results with those of Vukojevic et al.¹⁵ shows a large discrepancy in the relative magnitudes of I^- and Mn^{2+} components of the adjoint eigenvector; this difference needs further experimental clarification.

We regard our work as an initial study of the use of phase resetting methods in the elucidation of the kinetics of oscillating chemical reactions. This technique shows promise for further investigation of the Briggs–Rauscher reaction as well as in other oscillatory systems, such as the Belousov–Zhabotinsky reaction.

Acknowledgment. This work was supported in part by the Engineering Research Program of the Office of Basic Energy Sciences at the Department of Energy and the National Science Foundation.

References and Notes

- (1) Eiswirth M.; Freund A.; Ross J. *Adv. Chem. Phys.* **1991**, *43*, 1.
- (2) Strasser P.; Stemwedel, J. D.; Ross J. *J. Phys. Chem.* **1993**, *97*, 2851.
- (3) Stemwedel, J. D.; Ross, J. *J. Phys. Chem.* **1993**, *97*, 2863.
- (4) Chevalier T.; Schreiber, I.; Ross, J. *J. Phys. Chem.* **1993**, *97*, 6776.
- (5) Stemwedel, J. D.; Schreiber, I.; Ross, J. *Adv. Chem. Phys.* **1995**, *89*, 327.
- (6) Arkin, A.; Ross, J. *J. Phys. Chem.* **1995**, *99*, 970.
- (7) Hung Y. F.; Schreiber, I.; Ross J. *J. Phys. Chem.* **1995**, *99*, 1980.
- (8) Hung, Y. F.; Schreiber, I.; Ross, J. *J. Phys. Chem.* **1996**, *100*, 8556.
- (9) Arkin, A.; Shen, P.; Ross, J. *Science* **1997**, *277*, 1275.
- (10) Moran, F.; Vlad, M. O.; Ross, J. *J. Phys. Chem.* **1997**, *101*, 9410.
- (11) Sørensen, P. G.; Hynne, F. *J. Phys. Chem.* **1989**, *93*, 5467.
- (12) Hynne, F.; Sørensen, P. G.; Nielsen, K. *J. Chem. Phys.* **1990**, *92*, 1747.
- (13) Vance, W. N.; Ross J. *J. Chem. Phys.* **1995**, *103*, 2472.
- (14) Briggs, T. S.; Rauscher, W. C. *J. Chem. Educ.* **1973**, *50*, 496.
- (15) Vukojevic, V.; Sørensen, P. G.; Hynne, F. *J. Phys. Chem.* **1996**, *100*, 17175.
- (16) Turanyi, T. *React. Kinet. Catal. Lett.* **1991**, *45*, 235.
- (17) Furrow, S. D. *J. Phys. Chem.* **1987**, *91*, 2129.
- (18) We distinguish the perturbation strength q in quenching experiments from the perturbation amplitude ϵ in phase resetting experiments: q_k denotes the concentration increment of the k th species (for a δ function perturbation), whereas ϵ_k denotes a measure of the amplitude of a perturbation in the k th species that lasts one oscillation period.